HHS Public Access

Author manuscript

J Immunol. Author manuscript; available in PMC 2023 April 15.

Published in final edited form as:

J Immunol. 2022 April 15; 208(8): 1886–1900. doi:10.4049/jimmunol.2100743.

LincRNA-Cox2 functions to regulate inflammation in alveolar macrophages during acute lung injury

Elektra Kantzari Robinson[1], **Atesh Worthington**[1,2], **Donna Poscablo**[1,2], **Barbara Shapleigh**[1], **Mays Mohammed Salih**[1], **Haley Halasz**[1], **Lucas Seninge**[3], **Benny Mosqueira**[1], **Valeriya Smaliy**[1], **E. Camilla Forsberg**[2,3], **Susan Carpenter**[1,#]

[1]Department of Molecular, Cell and Developmental Biology, University of California Santa Cruz, 1156 High St, Santa Cruz, CA 95064

[2]Institute for the Biology of Stem Cells, University of California-Santa Cruz, Santa Cruz, California, United States of America

[3]Department of Biomolecular Engineering, University of California Santa Cruz, 1156 High St, Santa Cruz, CA 95064

Abstract

The respiratory system exists at the interface between our body and the surrounding non-sterile environment; therefore, it is critical for a state of homeostasis to be maintained through a balance of inflammatory cues. An appropriate inflammatory response is vital for combating pathogens, while an excessive or uncontrolled response can lead to the development of chronic disease. Recent studies have shown that actively transcribed noncoding regions of the genome are emerging as key regulators of biological processes, including inflammation. *LincRNA-Cox2* is one such example of an inflammatory inducible long intergenic noncoding RNA functioning to fine tune immune gene expression. Here using bulk and single-cell RNA-seq, in addition to fluorescence activated cell sorting, we identify that *lincRNA-Cox2* is most highly expressed in the lung, particularly in alveolar macrophages where it functions to regulate the acute inflammatory pathway. While we previously reported that *lincRNA-Cox2* can function to regulate its neighboring gene Ptgs2 in *cis*, here we use genetic mouse models to confirm its role in regulating gene expression more broadly in *trans*. We identify genes including Ccl3, Ccl4 and Ccl5 that are dysregulated in *lincRNA-Cox2* deficient mice. These genes are all rescued back to wild type levels by crossing the deficient mice with our newly generated *lincRNA-Cox2* transgenic mice confirming that this gene functions in *trans*. We confirm that many of these genes are specifically regulated within alveolar macrophages that originate in the bone marrow as the phenotype can be reversed by transplantation of wild type bone marrow into the *lincRNA-Cox2*

[#]Corresponding author: Susan Carpenter (sucarpen@ucsc.edu).

Author Contribution

E.K.R. designed, performed, and analyzed all molecular biology and *in vivo* experiments for all figures. A.W. and D.P. assisted with flow cytometry and sorting experiments, as well as helped design and perform chimera transplantation experiments. BS set-up and performed experiments for Figure 3. M.M.S., H.H. and S.C. assisted with all *in vivo* experiments. B.M. analyzed bulk RNA-sequencing experiments. V.S. helped with analyzing RT-qPCR experiments in Figure 5. L.S. analyzed all scRNA-sequencing datasets. E.C.F. helped with the design and analysis of B.M. transplantation and chimera experiments. E.K.R. and S.C. conceived and coordinated the project. E.K.R. and S.C. wrote the manuscript with input from all other co-authors.

Competing interests

The authors have no competing financial interests.

deficient mice. This work greatly expands our understanding of the role for *lincRNA-Cox2* in host defense and highlights the important role it plays in alveolar macrophages to regulate immune responses within the lung.

Introduction

Acute lung injury (ALI) and it's more severe form, known as acute respiratory distress syndrome (ARDS), are caused by dysregulated inflammatory responses resulting from conditions such as sepsis and trauma (1–5). Fundamentally, the characteristics of ALI include neutrophilic alveolitis, dysfunction of barrier properties, microvascular thrombosis, the formation of hyaline membrane, alveolar macrophage dysfunction, as well as indirect systemic inflammatory responses (6–9). Although a variety of anti-inflammatory pharmacotherapy are available, the morbidity and outcome of ALI/ARDS patients remain poor (10–13). Therefore, obtaining a more complete understanding of the molecular mechanisms that drive ALI inflammatory dysfunction is of great importance to improving both the diagnosis and treatment of the condition.

Long noncoding RNAs (lncRNAs) are a class of non-coding RNAs that include 18,000 in human and nearly 14,000 in the mouse genome (14, 15). Since their discovery, lncRNAs have been shown to be key regulators of inflammation both *in vitro* and *in vivo* (16, 17). Moreover, lncRNAs have also been characterized to be stable and detectable in body fluids (18), and therefore have enormous potential for biomarker discovery in both diagnosis and prognosis applications (19–21). Broadly, lncRNAs have been defined to function in *cis* to regulate their neighboring genes, as well as in *trans* to regulate genes on different chromosomes (16). A number of studies have been carried out to better understand the gene regulatory network between lncRNAs and mRNAs during ALI to identify novel biomarkers (22, 23). In addition to searching for biomarkers for ALI there have been studies performed to try and understand the functional mechanisms for lncRNAs during ALI (24). Lipopolysaccharide (LPS)-induced acute lung injury (ALI) is a commonly utilized animal model of ALI as it mimics the inflammatory induction and polymorphonuclear (PMN) cell infiltration observed during clinical ALI (25). One study showed that knocking down MALAT1, a well-studied lncRNA, exerts a protective role in the LPS induced ALI rat model and inhibited LPS-induced inflammatory response in murine alveolar epithelial cells and murine alveolar macrophages cells through sponging miR-146a (26). Additionally, Xist has been shown to attenuate LPS-induced ALI by functioning as a sponge for miR-146a-5p to mediate STAT3 signaling (27).

Previous work, by ourselves and others, identifies long intergenic noncoding RNA Cox2 (*lincRNA-Cox2*) as a regulator of immune cell signaling in macrophages (28–34). We have previously characterized multiple mouse models to show that *lincRNA-Cox2* functions *in vivo* to regulate the immune response. We showed that *lincRNA-Cox2* knockout mice (35) have profound defects in the neighboring protein coding gene Ptgs2. We went on to show that *lincRNA-Cox2* regulates Ptgs2 in *cis* through an enhancer RNA mechanism requiring locus specific transcription of the lncRNA (SFigure 1) (Elling *et al*, 2018). In order to study the function of *lincRNA-Cox2* independently of its role in regulating Ptgs2 in *cis* we

generated a *lincRNA-Cox2* mutant mouse using CRISPR to target the splice sites resulting in significant loss of the RNA allowing us to study the role for the RNA in *trans* (SFigure 1). We performed an LPS-induced endotoxic shock model and confirmed that *lincRNA-Cox2* is an important positive and negative regulator of immune genes in *trans*. We previously showed that *lincRNA-Cox2* is most highly expressed at steady-state in the lung and in this study (SFigure 1), we utilize our mutant model to determine if *lincRNA-Cox2* can function in *trans* to regulate gene expression in the lung (36). In addition, we characterize a transgenic overexpressing mouse model of *lincRNA-Cox2* (SFigure 1) and show that the defects in immune gene expression caused by removal of *lincRNA-Cox2* can be rescued by the overexpression of *lincRNA-Cox2* in an LPS-induced ALI model. On a cellular level, we show that *lincRNA-Cox2* is most highly induced following inflammation in alveolar macrophages where it functions to regulate signaling. Finally, we show through bone marrow chimeric studies that *lincRNA-Cox2* expression is coming from bone marrow derived cells to regulate genes within the lung. Collectively we show that *lincRNA-Cox2* is a *trans*-acting lncRNA that functions to regulate immune responses and maintain homeostasis within the lung at baseline and upon LPS-induced ALI.

Materials and Methods

Mice

Wild-type (WT) C57BL/6 mice were purchased from the Jackson Laboratory (Bar Harbor, ME) and bred at the University of California, Santa Cruz (UCSC). All mouse strains, including *lincRNA-Cox2* mutant (Mut), transgenic (Tg) and MutxTg mice, were maintained under specific pathogen-free conditions in the animal facilities of UCSC and protocols performed in accordance with the guidelines set forth by UCSC and the Institutional Animal Care and Use Committee.

Generation of *lincRNA-Cox2* Transgenic (Tg) and MutxTg Mice

lincRNA-Cox2 transgenic mice were generated by using a site-specific integrase-mediated approach described previously (37). In brief, TARGATT mice in the C57/B6 background contain a CAGG promoter within the Hipp11 (H11) locus expressing the full length *lincRNA-Cox2* (variant 1) as previously cloned (28) generated at the Gladstone (UCSF). These mice were then genotyped using the same TARGATT approach of PCR7/8 (PR432:GATATCCTTACGGAATACCACTTGCCACCTATCACC, SH176:TGGAGGAGGACAAACTGGTCAC, SH178:TTCCCTTTCTGCTTCATCTTGC). The *lincRNA-Cox2* transgenic mice were then crossed with the *lincRNA-Cox2* mutant mice and bred to homozygosity to generate MutxTG mice. For genotyping to assess homozygosity of Mutant we used the primer sets of MutF: ATGCCCAGAGACAAAAAGGA and MutR: GATGGCTGGATTCCTTTGAA, as well as the 3-primer set stated above.

ALI model

Age- and sex matched WT, *lincRNA-Cox2* mutant and *lincRNA-Cox2* MutxTG mice were treated with 3.5mg/kg using the oropharyngeal intratracheal administration technique. The model of LPS insult via oropharyngeal administration into the lung was previously described

in detail (38–40). Briefly, mice were sedated using an isoflurane chamber (3% for induction, 1–2% for maintenance), then 60–75ul of 3.5mg/kg of LPS (from strain O111:B4) or PBS (control) were administered using a pipette intratracheally. 24 h after LPS treatment, mice were sacrificed using CO2 and serum, BALF and lung were harvested for either cellular assessment by flow cytometry, RNA expression or sent to EVE technologies for cytokine/chemokine protein analysis.

LPS Shock model

Age- and sex matched wild-type, *lincRNA-Cox2* mutant mice, *lincRNA-Cox2* TG and *lincRNA-Cox2* MutxTG (36) (8–12 weeks of age) were injected i.p. with 20 mg/kg LPS (O111:B4). For gene expression analysis and cytokine analysis, mice were euthanized 6 h post injection. Blood was taken immediately postmortem by cardiac puncture. Statistics were performed using GraphPad prism.

Transplantation reconstitution Assays

Reconstitution assays were performed, as previously stated by Poscablo *et al.* (41), by transplanting double-sorted HSCs (3 million cells per recipient) from Ubc-GFP+ whole BM and transplanting into congenic C57BL/6 WT and *lincRNA-Cox2* deficient mice via retro-orbital intravenous transplant generating WT→WT and WT→Mut. Hosts were preconditioned with lethal radiation (~1050 rads) using a Faxitron CP160 X-ray instrument (Precision Instruments).

Harvesting Bronchiolar Lavage Fluid (BAL)

Bronchoalveolar Lavage Fluid (BALF) was harvested as previously stated by Cloonan *et al.* (42). 40 mice were euthanized by CO2 narcosis, the tracheas cannulated, and the lungs lavaged with 0.5-ml increments of ice-cold PBS eight times (4 ml total), samples were combined in 50 ml conical tubes. BALF was centrifuged at 500 *g* for 5 min. 1 ml red blood cell lysis buffer (Sigma-Aldrich) was added to the cell pellet and left on ice for 5 min followed by centrifugation at 500 *g* for 5 min. The cell pellet was resuspended in 500 μl PBS, and leukocytes were counted using a hemocytometer. Specifically, 10 μl was removed for cell counting (performed in triplicate) using a hemocytometer. Cells were plated in sterile 12 well plates at 5e5/well (total of 8 wells) and use complete DMEM with 25 ng/ml supGM-CSF.

Lung Tissue Harvesting for cytokine measurement

Mice were humanely sacrificed, and their lungs were excised. The whole lungs were snap frozen and homogenized, and the resulting homogenates were incubated on ice for 30 min and then centrifuged at 300 × *g* for 20 min. The supernatants were harvested, passed through a 0.45-μm-pore-size filter, and used immediately or stored at −70°C, then sent to EVE for measurements of cytokines/chemokines.

Cell culture of Primary AMs

BALF isolation performed on 10 WT and 10 *lincRNA-Cox2* mutant mice, cells were pooled, counted and plated. 24 h post-BALF isolation, media was removed and fresh complete

DMEM with 25 ng/ml supGM-CSF is added (43). All cells that adhere to the surface of the plate are considered alveolar macrophages (AM) as previously determined by Chen *et al.* (44). After new media is added, AMs are stimulated with 200 ng/ml LPS (Sigma, L2630–10MG). Harvest supernatant 6 h post-stimulation. Harvested supernatant was sent to Eve technologies for cytokine analysis. Experiment was performed twice, utilizing a total of 40 mice. Statistics were performed using GraphPad prism.

RNA isolation, cDNA synthesis and RT-qPCR

Total RNA was purified from cells or tissues using Direct-zol RNA MiniPrep Kit (Zymo Research, R2072) and TRIzol reagent (Ambion, T9424) according to the manufacturer's instructions. RNA was quantified and assessed for purity using a nanodrop spectrometer (Thermo Fisher). Equal amounts of RNA (500 to 1,000 ng) were reverse transcribed using iScript Reverse Transcription Supermix (Bio-Rad, 1708841), followed by qPCR using iQ SYBR Green Supermix reagent (Bio-Rad, 1725122) with the following parameters: 50 °C for 2 min and 95 °C for 2 min, followed by 40 cycles of 95 °C for 15 s, 60 °C for 30 s, and 72 °C for 45 s, followed by melt-curve analysis to control for nonspecific PCR amplifications. Oligos used in qPCR analysis were designed using Primer3 Input version 0.4.0 (https://bioinfo.ut.ee/primer3–0.4.0/).

Gene expression levels were normalized to Gapdh or Hprt as housekeeping genes.

Primers Used:

Gapdh F- CCAATGTGTCCGTCGTGGATC

Gapdh R - GTTGAAGTCGCAGGAGACAAC

Hprt F - TGCTCGAGATGTCATGAAGG

Hprt R - ATGTCCCCCGTTGACTGAT

lincRNACox2 F - AAGGAAGCTTGGCGTTGTGA

lincRNACox2 R - GAGAGGTGAGGAGTCTTATG

ELISA

The concentration of Il6 and Ccl5 levels in the serum and BAL of WT, *lincRNA-Cox2* mutant mice, *lincRNA-Cox*2 Tg *and lincRNA-Cox2* MutxTg mice were determined using the DuoSet ELISA kits (R&D, DY1829 and DY478) according to the manufacturer's instructions.

Lung Tissue Harvesting for Cellular Analysis

Mice were humanely sacrificed, and their lungs were excised. Lung was inflated with a digestion solution containing 1.5mg/ml of Collagenase A (Roche) and 0.4mg/ml DNaseI (Roche) in HBSS plus 5% fetal bovine serum and 10mM HEPES. Trachea was tied off with 2.0 sutures. The heart and mediastinal tissues were carefully removed, and the lung parenchyma placed in 5ml of digestion solution and incubated at 37°C for 30 minutes

with gently vortexing every 8–10 minutes. Upon completion of digestion, 25ml of PBS was added; and the samples were vortexed at maximal speed for 30 seconds. The resulting cell suspensions were strained through a 70um cell strainer and treated with ACK RBC lysis solution. Then the cells were stained using the previously published immune (45) and epithelial (46) cellular panels.

Flow Cytometry Analysis and Sorting

After cells were isolated and counted, ~2×10^6 cells per sample were incubated in blocking solution containing 5% normal mouse serum, 5% normal rat serum, and 1% FcBlock (eBiosciences) in PBS and then stained with a standard panel of immunophenotyping antibodies (Supplemental Tables 2: list of antibodies, clones, fluorochromes, and manufacturers) for 30 minutes at room temperature (45). Data was acquired and compensation was performed on the BD Aria II and Attune NxT (Thermo Fisher) flow cytometer at the beginning of each experiment. Data was analyzed using Flowjo v10. Cell sorting was performed on a BD Aria II. The collected cells were harvested for RNA and RT-qPCR was performed to measure *lincRNA-Cox2*. Analysis was performed using FlowJo analysis software (BD Biosciences).

RNA-sequencing Analysis

Generation of the RNAseq data (GSE117379 and GSE94749) and analysis of differential gene expression has been described previously (36, 47). RNA-seq 50bp or 30bp, respectively, reads were aligned to the mouse genome (assembly GRCm38/mm10) using TopHat. The Gencode M13 gtf was used as the input annotation. Differential gene expression specific analyses were conducted with the DESeq2 R package. Specifically, DESeq2 was used to normalize gene counts, calculate fold change in gene expression, estimate p-values and adjusted p-values for change in gene expression values, and to perform a variance stabilized transformation on read counts to make them amenable to plotting.

single cell RNA-sequencing Analysis

Generation of the sc-RNAseq data (Gene Expression Omnibus accession number GSE120000 and GSE113049) and analysis of gene expression has been described previously (48, 49). All analysis was performed using the Scanpy package (50). Unless specified, default parameters were used.For GSM3391587:Count matrix was processed according to the original study. Briefly, the count matrix was normalized to log(10K+1) transcripts, and highly variable genes were selected with the following parameters: minimum dispersion=0.2, minimum mean=0.15. Those genes were used to compute principal components, out of which the top 6 were selected for clustering and visualization. t-SNE coordinates were computed using the top 6 PCs, and louvain clustering was performed based on the k-nearest neighbor graph (k=30) derived from the principal components. For GSE113049:Count matrix was processed as follows: Cells with less than 200 detected genes were removed, and genes detected in less than 3 cells were removed. Cells with more than 5% of mitochondrial content were further excluded from the analysis. Counts were normalized to log(10K+1) transcripts. t-SNE coordinates, and cell type labels were obtained from public files made available by the authors of the original study.

Results

Immune gene expression is altered in the lungs of lincRNA-Cox2 deficient mice.

In order to determine the role for *lincRNA-Cox2* in the lung we first examined RNA-sequencing data of Wild type (WT) versus *lincRNA-Cox2* mutant mice treated with PBS to compare gene expression profiles (36) (Figure 1A). We found 85 genes down-regulated and 41 genes up-regulated in the *lincRNA-Cox2* mutant lungs compared to WT (Figure 1B, STable 1). Gene-ontology analysis showed that both the down and up regulated genes were associated with the immune system, metabolism, and response to stimulus (Figure 1C–D), which are similar to pathways that *lincRNA-Cox2* has previously been associated with in bone marrow derived macrophages (BMDMs) (28). To determine if loss of *lincRNA-Cox2* impacts protein expression we performed ELISAs on lung homogenates from WT and *lincRNA-Cox2* deficient mice (Figure 1E). While many genes remained unchanged at baseline (PBS) between the WT and *lincRNA-Cox2* mutant lungs (SFigure 2A–H), we did find that Il-12p40, Cxcl10, Ccl3, Ccl4, Cxcl2, Ccl5 and Ccl19 are all significantly up-regulated in the mutant lungs (Figure 1F–L). Interestingly, none of these cytokines are up-regulated at the RNA level in our whole lung tissue RNA-sequencing suggesting that they might be regulated post-transcriptionally or that they are only regulated in a small subset of cells that cannot be easily captured from the whole lung lysate RNA-seq data (SFigure 2I–P).

Finally, we measured the immune cell repertoire in the bronchiolar lavage fluid (BAL) of WT and *lincRNA-Cox2* deficient mice and found that B cells and dendritic cells, while at very low expression levels in both strains, are significantly lower at baseline in the mutant mice (Figure 1M). These findings indicate that *lincRNA-Cox2* functions as both a positive and negative regulator of immune gene expression which can impact the cellular milieu within the lung at steady-state in mice.

LincRNA-Cox2 regulates the pro-inflammatory response during acute lung injury (ALI).

Our data suggests that *lincRNA-Cox2* plays a role in regulating immune gene expression at steady-state, therefore we wanted to determine if loss of *lincRNA-Cox2* could impact the immune response during acute lung injury. We employed a 24 h LPS induced acute lung injury (ALI) model, since *lincRNA-Cox2* is highly expressed at this timepoint (Figure 2A–B). We assessed the immune cell repertoire within the BAL by flow cytometry in WT and *lincRNA-Cox2* mutant mice following LPS challenge and found that the most abundant and critical cell type, neutrophils, were significantly reduced when *lincRNA-Cox2* was removed (Figure 2C). We also assessed the cytokine and chemokine response both in the BAL and serum of WT and *lincRNA-Cox2* mutant mice by ELISA. We found that Il6, Ccl3 and Ccl4 were downregulated in the serum and the BAL of the *lincRNA-Cox2* mutant mice (Figure 2D–F). In addition, several proteins were specifically affected either in the serum or BAL, such as Ccl5 and Ccl22 which were upregulated in the serum (Figure 2G–H), while Ifnb1 was upregulated only in the BAL of the mutant mice (Figure 2I). Consistent with our previous work, Tnfa remains unchanged between WT and *lincRNA-Cox2* mutant mice (Figure 2J). These data suggest that *lincRNA-Cox2* exerts different effects within the lung

compared to the periphery and that *lincRNA-Cox2* can impact acute inflammation at the protein and cellular levels within the lung.

Generation and characterization of a transgenic mouse model overexpressing lincRNA-Cox2.

We have determined that *lincRNA-Cox2* is critical in regulating inflammation at baseline, during a septic shock model (36) and here during an acute lung injury model. In order to confirm that *lincRNA-Cox2* is functioning in *trans*, we generated a transgenic *lincRNA-Cox2* mouse line using the TARGATT system, which allows for stable integration of *lincRNA-Cox2* into the H11 locus (37) (Figure 3A). The inserted cassette is carrying a CAG promoter, *lincRNA-Cox2*, and an SV40 polyA stop cassette. Mice were bred to homozygosity (SFigure 3A–D), and *lincRNA-Cox2* levels were measured in WT and Transgenic bone-marrow-derived macrophages (BMDMs) (Figure 3B). As expected, *lincRNA-Cox2* is highly expressed in the transgenic macrophages with no difference in expression following LPS stimulation (Figure 3B).

Next, we performed a septic shock model of WT and transgenic mice to determine if overexpression of *lincRNA-Cox2* can impact the immune response (Figure 3C). As expected *lincRNA-Cox2* is highly expressed in the lung tissue of the transgenic mice and interestingly we observe increased levels of Il6 while other *lincRNA-Cox2* target genes, such as Ccl5 are not affected. This suggests that overexpression of *lincRNA-Cox2* can have the opposite phenotype to knocking out the gene to regulate Il6 within the lung (Figure 3D, SFigure 3E–G). We harvested serum from the mice and found higher levels of Csf1 and lower levels of Il10 (Figure 3E–F) in the mice overexpressing *lincRNA-Cox2*. Other inflammatory cytokines including Il6, Ccl5, Ccl3 and Ccl4 were unaltered in *lincRNA-Cox2* transgenic mice serum (Figure 3G–J, SFigure 3H–K). These data suggests that overexpression of *lincRNA-Cox2* does not have broad impacts on gene expression during acute systemic inflammation.

Next, we assessed whether overexpression of *lincRNA-Cox2* dysregulated the inflammatory responses within the lung by utilizing the LPS induced acute lung injury model (Figure 4A). First, we performed RT-qPCR and confirmed that the overexpression of *lincRNA-Cox2* did not alter the expression of Ptgs2 in the BAL consistent with our previously findings that it is regulated in *cis* and not in *trans* (Figure 4B–C) (36). To assess the function of *lincRNA-Cox2* in the lung, we then measured the immune cell repertoire within the BAL by flow cytometry in WT and *lincRNA-Cox2* TG mice following LPS challenge and found no significant difference in cell numbers (Figure 4D). Finally, utilizing both BAL and serum we measured the cytokine and chemokine profiles of WT and *lincRNA-Cox2* TG mice by ELISA. Interestingly, we found that overexpression of *lincRNA-Cox2* resulted in an upregulation of Il6, and Ccl3 (Figure 4E–F) in the BAL following ALI which is the opposite phenotype to the deficient mice (Figure 2). Ccl4 levels trend upwards, but do not reach significance (Figure 4G). The *lincRNA-Cox2* transgenic mice also showed a specific down-regulation in Timp1 in the BAL during ALI (Figure 4H) and an upregulation of Il10 (Figure 4I) in the serum. Consistent with knocking-down *lincRNA-Cox2*, overexpressing this gene did not alter the regulation of Tnf in either the BAL or in the serum (Figure 4J).

These data suggest that *lincRNA-Cox2* functions in *trans* to regulate immune genes during acute inflammation.

LincRNA-Cox2 functions in trans to regulate acute inflammation.

To confirm that *lincRNA-Cox2* is regulating genes *in trans* following *in vivo* challenge with LPS we crossed the mice deficient in *lincRNA-Cox2* (Mut) with the transgenic mice overexpressing *lincRNA-Cox2* (TG) generating mice labeled throughout as MutxTG (Figure 5A, SFigure 4A–B). We first performed an intraperitoneal (IP) endotoxic shock model to determine if we could rescue the *lincRNA-Cox2* phenotype identified in our previous study (36) (Figure 5B). As expected, *lincRNA-Cox2* expression is significantly reduced in the lung tissue and BAL of the deficient mice (Mut) mice, and highly expressed in the MutxTG mouse (Figure 5C–D). We found that Ccl5 and Cxcl10 are expressed at higher levels in the BAL and serum of *lincRNA-Cox2* mutant mice (Figure 5E–H) and the expression levels can be rescued by trans expression of *lincRNA-Cox2* in the MutxTG mice returning to WT levels.

Next, we wanted to determine if transgenic overexpression of *lincRNA-Cox2* can reverse the phenotype observed in the deficient mice during acute lung injury (Figure 6A). We assessed immune cell recruitment in both the BAL and lung tissue by flow cytometry in WT, mutant and MutxTG mice. Again, we found that neutrophils are the only immune cell that was significantly lower in *lincRNA-Cox2* mutant mice, while neutrophil recruitment in MutxTG mice was rescued and returned to WT levels (Figure 6B–C). Next, we performed ELISAs on harvested lung tissue, BAL and serum to measure the protein concentration of cytokines and chemokines. We found that Il6, Ccl5, Ccl3, Ccl4, Ccl22 and Ifnb1 are consistently significantly dysregulated in the *lincRNA-Cox2* mutant mice and again this phenotype could be rescued back to WT levels by the transgenic overexpression of *lincRNA-Cox2* (MutxTG) (Figure 6D–I). Interestingly, Il6, Ccl3, Ccl4 and Ifnb1 are all significantly different in the BAL, while Ccl5 and Ccl22 are only significantly dysregulated in the lung tissue suggesting that *lincRNA-Cox2* can impact proteins in a cell-specific manner. These cytokines are not significantly altered at the transcript level (SFigure 4C–E). We found that Tnf is consistently unaltered between all genotypes (Figure 6J). From these data we conclude that *lincRNA-Cox2* functions in *trans* to regulate the lung immune response during acute inflammation.

LincRNA-Cox2 positively and negatively regulates immune genes in primary alveolar macrophages.

In order to understand how *lincRNA-Cox2* could be regulating acute inflammation we first wanted to determine which cell types *lincRNA-Cox2* is most highly expressed within the lung. First, we utilized publicly available single-cell RNA sequencing (scRNA-seq) data from two LPS-induced lung injury studies (48, 49). Overall, *lincRNA-Cox2* expression was very low in these datasets (SFigure 5A–E). There was a slight increase in expression in all alveolar epithelial type 2 (ATII) cellular populations (SFigure 5D–E). Due to the expression level limitations of publicly available scRNA-seq datasets, we next performed fluorescence activated cell sorting (FACS) to isolate all cell-types of interest in the lung at baseline and following LPS-induced lung injury (36). Using RT-qPCR we found that *lincRNA-Cox2* was most highly expressed in neutrophils at both baseline and following LPS stimulation

when normalized to cell count (SFigure 5F–G). Interestingly alveolar macrophages (AMs) were identified as the cell type with the highest induction of *lincRNA-Cox2*, following LPS stimulation (Figure 7A).

Since *lincRNA-Cox2* is most highly induced in AMs we wanted to determine if this was the cell type contributing to the cytokine and chemokine changes in *lincRNA-Cox2* deficient (Mut) mice following inflammatory challenge. To do this, we harvested BAL fluid from WT and *lincRNA-Cox2* mutant mice to culture primary alveolar macrophages and treated them with LPS for 24 h (Figure 7B). First, *lincRNA-Cox2* induction was validated using RT-qPCR with *in vitro* LPS stimulated WT AMs while expression as expected is diminished in the *lincRNA-Cox2* deficient AMs (Figure 7B–C). Finally, we assessed the level of cytokine and chemokine expression from primary AMs by ELISA. We confirmed significant dysregulation of Il6, Ccl5, Ccl3, Ccl4 and Ccl22 in primary alveolar macrophages, which are consistent with the *in vivo* data (Figure 6D–H). Performing RT-qPCR on primary AMs we found that these cytokines are not significantly dysregulated at the level of transcription (SFigure 5H–K). Additionally, we found novel dysregulation of Cxcl2, Cxcl1, Cxcl10 specific to alveolar macrophages from the *lincRNA-Cox2* deficient mice not detected in our ALI model. Tnf remains consistently unchanged between WT and mutant in AMs and *in vivo* studies (Figure 7M). These data indicate that mechanistically *lincRNA-Cox2* is functioning to regulate protein expression primarily within primary alveolar macrophages.

Peripheral immune cells drive the regulatory role of lincRNA-Cox2 during ALI.

From our *in vivo* mouse models, we can conclude that *lincRNA-Cox2* functions in *trans* to regulate immune genes and cellular milieu within the lung during ALI. Utilizing previously generated data of sorted resident and recruited AMs from mice exposed to LPS induced ALI (SFigure 6A) from Mould *et al.* (47), we found that *lincRNA-Cox2* is expressed in both cell types. When comparing the AM subsets, we found that *lincRNA-Cox2* was more highly expressed in recruited AMs at day 3 of ALI (SFigure 6B).

To determine if *lincRNA-Cox2* functions through bone-marrow derived immune cells, we performed bone marrow (BM) transplantation experiments utilizing Ubiquitin C (Ubc)-GFP WT bone marrow to enable us to easily track chimerism through measurement of GFP. Ubc-GFP WT BM was transplanted into *lincRNA-Cox2* mutant mice and WT mice generating WT→WT and WT→Mut mice (Figure 8A). First, we determined the reconstitution of HSCs by measuring donor chimerism (GFP%) in the peripheral blood (PB) for the duration of the 8 weeks. We found that both the WT→WT and WT→Mut mice have 100% donor reconstitution of granulocytes/ myelomonocytes (GMs) and B cells and ~75% donor T cells in peripheral blood (Figure 8B–D). While there was a small but significant decrease in T cell reconstitution in WT→Mut mice, we found there is no significant reconstitution difference of GMs or B cells between WT→WT and WT→Mut mice.

After 8 weeks when the immune system was fully reconstituted, we performed the LPS ALI model on the chimera WT→WT and WT→Mut mice. We found that the percentage of donor reconstitution within peripheral blood was 100% indicating a successful BM transplantation (Figure 8B–D, SFigure 6C–K) (51). We found that the decrease in neutrophil recruitment that we identified in the *lincRNA-Cox2* mutant mice (Figure 2B, Figure 6B–

C, Figure 7E, SFigure 6L) were rescued in the WT→Mut model back to similar levels to the WT→WT mice (Figure 8E). Furthermore, the altered expression of Il6, Ccl3, and Ccl4 found in the *lincRNA-Cox2* mutant mice were also returned to WT levels in the WT→Mut mice (Figure 2C–E, Figure 6D–F, Figure 8F–H). As expected, Tnf acts as a control cytokine showing no difference across genotypes (Figure 8I). These data suggest that *lincRNA-Cox2* is functioning through an immune cell from the bone marrow, most likely alveolar macrophages to regulate acute inflammatory responses within the lung.

Discussion

LncRNAs are rapidly emerging as critical regulators of biological responses and in recent years there have been several studies showing that these genes play key roles in regulating the immune system (16). However very few studies have functionally characterized lncRNAs using mouse models *in vivo*. We and others have studied the role for *lincRNA-Cox2* in the context of macrophages and shown that it can act as both a positive and negative regulator of immune genes (28–34). We previously characterized two mouse models of *lincRNA-Cox2*, a knockout (KO) and an intronless splicing mutant (Mut). We identified *lincRNA-Cox2* as a *cis* acting regulator of its neighboring protein coding gene Ptgs2 using the KO mouse model. In order to study the role for *lincRNA-Cox2* independent of its *cis* role regulating Ptgs2 we generated the splicing mutant (Mut) mouse model (SFigure 1). This model enabled us to show that knocking down *lincRNA-Cox2* impacts a number of immune genes including Il6 and Ccl5 in an LPS induced endotoxic shock model (36). In this current study we make use of the mutant mouse model to study the role for *lincRNA-Cox2* in regulating immune responses in the lung, where *lincRNA-Cox2* is most highly expressed, both at steady-state and following LPS-induced acute lung injury (ALI). Both neutrophil recruitment and chemokine/cytokine induction are hallmarks of acute lung injury (ALI) (38, 52, 53) and here we provide *in vivo* and *in vitro* evidence that *lincRNA-Cox2* plays an important role in these processes.

We found that loss of *lincRNA-Cox2* at baseline resulted in the up- and down-regulation of a number of genes that regulate the immune system and metabolism (Figure 1A–D) indicating that *lincRNA-Cox2* is a key transcriptional regulator of gene expression within lung tissue. In addition, we measured immune cells and found that at baseline dendritic cells and B cells were lower in the *lincRNA-Cox2* mutant mice. Lung DCs serve as a functional signaling/sensing units to maintain lung homeostasis by orchestrating host responses to benign and harmful foreign substances, while B cells are crucial for antibody production, antigen presentation and cytokine secretion (23, 54). Having fewer DC and B cells at steady state could lead to an increased risk of inflammatory diseases (55, 56). This indicates that *lincRNA-Cox2* plays an important role in maintaining lung homeostasis since gene expression and cellular abundance are altered by the loss of *lincRNA-Cox2*.

While we identify *lincRNA-Cox2* as a crucial element for maintaining lung homeostasis, we next performed LPS induced acute lung injury (ALI) to assess the importance of *lincRNA-Cox2* during active inflammation. Using a 24 h time point, which shows the maximum influx of polymorphonuclear cells (PMNs) and cytokine/chemokine expression and highest expression of *lincRNA-Cox2* (Figure 2A) (52), we found that loss of *lincRNA-Cox2* led

to a decrease in neutrophil recruitment and altered cytokine/chemokine expression in both the BAL and serum (Figure 2). In acute lung injury, neutrophils are crucial for bacterial clearance during live infection, repair and tissue remodeling after ALI (57, 58). Our data suggests that *lincRNA-Cox2* plays an important role in neutrophil recruitment and therefore could also play roles in clearance of live bacteria and repair of tissue after resolution of infection. We found that Il6 levels were reduced while Ccl5 levels were increased following ALI in the *lincRNA-Cox2* mutant mice. These findings are consistent with our previous *in vitro* and *in vivo* studies (28, 36). In addition, we found that Ccl3 and Ccl4 are positively regulated, while Ccl22 and Ifnb1 are negatively regulated by *lincRNA-Cox2* in the lung during ALI. Interestingly, Lee *et al.* and others have reported that the chemokines, CCL3 and CCL4, promote the local influx of neutrophils (59–63). Therefore, the decreased expression of Ccl3 and Ccl4 *in vivo* in the *lincRNA-Cox2* mutant mice could explain the significant decrease of neutrophil recruitment seen in the BAL (Figure 2B).

To date there remains only a small number of lncRNAs that have been functionally and mechanistically characterized *in vivo*. In fact, Pnky, Tug1 and Firre are the only other lncRNA studies that show that their phenotype can be rescued in *trans in vivo* (64–66). From our previous *in vivo* studies, we had concluded that *lincRNA-Cox2* functions in *cis* to regulate Ptgs2 in an eRNA manner while it functions in *trans* to regulate genes such as Il6 and Ccl5 (36). In order to prove that indeed *lincRNA-Cox2* can function in *trans* to regulate immune genes we generated a transgenic mouse overexpressing *lincRNA-Cox2* from the H11 locus using the TARGATT system (37) (Figure 3A, SFigure 1). Simply overexpressing *lincRNA-Cox2* minimally impacts the immune response following an LPS septic shock model, but widely impacts genes utilizing an LPS induced ALI model suggesting that *lincRNA-Cox2* is an important regulator of immune genes within the lung (Figure 3–4). Using the septic shock model, we do note that Csf1 and Il10 are lower in serum following endotoxic shock in the *lincRNA-Cox2* transgenic mouse. However, in the ALI model overexpression of *lincRNA-Cox2* resulted in an increase in Il6 and Ccl3 production within the BAL (Figure 4) which is the opposite phenotype to that observed when *lincRNA-Cox2* is removed (Figure 2). Unique to the overexpression of *lincRNA-Cox2* was the decreased levels of Timp1 and previous work indicates that dysregulation of Timp1 in the lungs is critical to resolution of lung injury, as well as evading live pathogen infection (38, 67–69). These data suggest that overexpression of *lincRNA-Cox2 in vivo* could be in important model to study specific aspects of lung immune regulation.

Our primary goal for generating the transgenic mouse line overexpressing *lincRNA-Cox2* was to determine if crossing it to our *lincRNA-Cox2* mutant (deficient) mouse generating a MutxTG line (Figure 5A) would rescue the phenotypes observed in the mutant line following LPS challenge using either an intraperitoneal delivery or via oropharyngeal delivery. Interestingly, we found that our MutxTG mice do rescue the phenotype found in both the endotoxic shock model (Figure 5) and LPS induced ALI model (Figure 6), showing definitively that *lincRNA-Cox2* regulates specific genes as well as neutrophil recruitment in *trans*. Further work will need to be carried out in order to determine if *lincRNA-Cox2* is functioning directly to regulate specific genes or if it is indirect.

To delve more deeply into exactly how *lincRNA-Cox2* functions to regulate immune genes in the lung we focused on determining which cell type *lincRNA-Cox2* is most highly expressed in. Analysis of scRNA-seq indicated that *lincRNA-Cox2* was highly expressed in naive and injured alveolar epithelial type II (AECII) cells (SFigure 5A–E), however overall *lincRNA-Cox2* was difficult to detect in single-cell data probably due to a combination of low expression levels and low read depth. Utilizing FACS and qRT-PCR, we measured the expression of *lincRNA-Cox2* in 8 immune cell populations and 4 epithelial/endothelial cell populations and found that *lincRNA-Cox2* was most highly expressed in neutrophils (SFigure 5F–G). However, when assessing induction of *lincRNA-Cox2* following LPS and normalizing to PBS controls we found it to be most highly expressed in alveolar macrophages with some significant induction also observed in monocytes (Figure 7A). We know alveolar macrophages are critical effector cells in initiating and maintaining pulmonary inflammation, as well as termination and resolution of pulmonary inflammation during acute lung injury (ALI) (70, 71). Therefore, to determine if the altered gene expression profiles we observed within the BAL following ALI were due to *lincRNA-Cox2* expression in alveolar macrophages we cultured primary alveolar macrophages using previously published methods (43, 72, 73) from our WT and *lincRNA-Cox2* mutant mice and measured cytokine and chemokine expression. Excitingly, we found decreased expression of Il6, Ccl3 and Ccl4 and increased expression of Ccl5 in the *lincRNA-Cox2* mutant alveolar macrophages (Figure 7D–G) consistent with our *in vivo* findings from the BAL following ALI. Several other chemokines such as Ccl3, Ccl4, Csf3, Cxcl1 and Cxcl2 were significantly lower in the *lincRNA-Cox2* deficient alveolar macrophages and these all are known to play roles in neutrophil influx (59, 61, 74). These data suggest that *lincRNA-Cox2* functions within alveolar macrophages to regulate gene expression including key chemokines that can impact neutrophil infiltration during acute lung injury.

During ALI many of the immune cells that infiltrate the lung, including some classes of alveolar macrophages, originate from the bone marrow. Analysis of resident and recruited alveolar macrophages during ALI, showed *lincRNA-Cox2* is more highly expressed in recruited (bone marrow derived) alveolar macrophages (SFigure 6A–B). Therefore, to assess if *lincRNA-Cox2* is functioning through bone marrow (BM) derived immune cells we performed BM transplantation chimera experiments in WT and *lincRNA-Cox2* mutant mice (Figure 7A). We found that WT→Mut BM transplantations completely rescued the neutrophil and cytokine/chemokine phenotype in the BAL (Figure 8B–H, SFigure 6L). While we aimed to determine if *lincRNA-Cox2* functions either through resident (SiglecF+) or recruited (Siglec F-) alveolar macrophages, we found that both populations were composed of >70% donor BM (SFigure 6J–K) indicating that radiation obliterated resident SiglecF+ alveolar cells which become repopulated with donor cells from the bone marrow (51, 75–78). These experiments enabled us to conclude that *lincRNA-Cox2* expression originating from the bone marrow, can function to control immune responses in the lung, since BM derived immune cells transplanted into *lincRNA-Cox2* mutant mice are able to rescue the phenotype driven by loss of *lincRNA-Cox2* in the lung. While these data do rule out epithelial cells as a source of the *lincRNA-Cox2* mediated phenotype we did not examine any role for *lincRNA-Cox2* in other immune infiltrating cells such as neutrophils

and therefore cannot definitively rule them out as playing some role in addition to the alveolar macrophages.

In conclusion, in this study we show, through multiple mouse models, that *lincRNA-Cox2* is functioning in *trans* in alveolar macrophages to regulate immune responses within the lung. This study provides an additional layer of mechanistic understanding highlighting that lncRNAs can contribute to the delicate balance between maintenance of homeostasis and induction of transient inflammation within the lung microenvironment.

Supplementary Material

Refer to Web version on PubMed Central for supplementary material.

Acknowledgments

We thank the UCSC Flow Cytometry Core Facility, RRID:SCR_021149, for technical assistance. Additionally, we thank Biorender for creating a platform to easily generate figures using "Biorender.com".

Funding

This work was partially supported by the California Tobacco related disease research fund to SC (27IP-0017H). This work was supported by CIRM Facilities awards CL1-00506 and FA1-00617-1 to UCSC. E.K.R. was supported by the NIH Predoctoral Training Grant (T32 GM008646). This work was funded a Howard Hughes Medical Institute Gilliam Fellowship Award, and an American Heart Association Predoctoral Fellowship Award to D.P.; by an NIH NHLBI F31 Fellowship Award and a Tobacco-Related Disease Research Program Predoctoral Fellowship Award to A.W.

References

1. Moldoveanu B, Otmishi P, Jani P, Walker J, Sarmiento X, Guardiola J, Saad M, and Yu J. 2009. Inflammatory mechanisms in the lung. J Inflamm Res 2: 1–11. [PubMed: 22096348]
2. Mokra D, and Kosutova P. 2015. Biomarkers in acute lung injury. Respir Physiol Neurobiol 209: 52–58. [PubMed: 25466727]
3. Wang Y-C, Liu Q-X, Zheng Q, Liu T, Xu X-E, Liu X-H, Gao W, Bai X-J, and Li Z-F 2019. Dihydromyricetin Alleviates Sepsis-Induced Acute Lung Injury through Inhibiting NLRP3 Inflammasome-Dependent Pyroptosis in Mice Model. Inflammation 42: 1301–1310. [PubMed: 30887396]
4. Mowery NT, Terzian WTH, and Nelson AC 2020. Acute lung injury. Curr Probl Surg 57: 100777.
5. Butt Y, Kurdowska A, and Allen TC 2016. Acute Lung Injury: A Clinical and Molecular Review. Arch Pathol Lab Med 140: 345–350. [PubMed: 27028393]
6. Pittet JF, Mackersie RC, Martin TR, and Matthay MA 1997. Biological markers of acute lung injury: prognostic and pathogenetic significance. Am J Respir Crit Care Med 155: 1187–1205. [PubMed: 9105054]
7. Alluri R, Kutscher HL, Mullan BA, Davidson BA, and Knight PR 2017. Open Tracheostomy Gastric Acid Aspiration Murine Model of Acute Lung Injury Results in Maximal Acute Nonlethal Lung Injury. J Vis Exp.
8. Gouda MM, and Bhandary YP 2019. Acute Lung Injury: IL-17A-Mediated Inflammatory Pathway and Its Regulation by Curcumin. Inflammation 42: 1160–1169. [PubMed: 31011925]
9. Fan EKY, and Fan J. 2018. Regulation of alveolar macrophage death in acute lung inflammation. Respir Res 19: 50. [PubMed: 29587748]
10. Raghavendran K, Pryhuber GS, Chess PR, Davidson BA, Knight PR, and Notter RH 2008. Pharmacotherapy of acute lung injury and acute respiratory distress syndrome. Curr Med Chem 15: 1911–1924. [PubMed: 18691048]

11. Yin J, and Bai C-X 2018. Pharmacotherapy for Adult Patients with Acute Respiratory Distress Syndrome. Chin Med J (Engl) 131: 1138–1141. [PubMed: 29722332]
12. Suo T, Chen G-Z, Huang Y, Zhao K-C, Wang T, and Hu K. 2018. miRNA-1246 suppresses acute lung injury-induced inflammation and apoptosis via the NF-κB and Wnt/β-catenin signal pathways. Biomed Pharmacother 108: 783–791. [PubMed: 30253370]
13. Deng G, He H, Chen Z, OuYang L, Xiao X, Ge J, Xiang B, Jiang S, and Cheng S. 2017. Lianqinjiedu decoction attenuates LPS-induced inflammation and acute lung injury in rats via TLR4/NF-κB pathway. Biomed Pharmacother 96: 148–152. [PubMed: 28972887]
14. Uszczynska-Ratajczak B, Lagarde J, Frankish A, Guigó R, and Johnson R. 2018. Towards a complete map of the human long non-coding RNA transcriptome. Nat Rev Genet 19: 535–548. [PubMed: 29795125]
15. Fang S, Zhang L, Guo J, Niu Y, Wu Y, Li H, Zhao L, Li X, Teng X, Sun X, Sun L, Zhang MQ, Chen R, and Zhao Y. 2018. NONCODEV5: a comprehensive annotation database for long non-coding RNAs. Nucleic Acids Res 46: D308–D314. [PubMed: 29140524]
16. Robinson EK, Covarrubias S, and Carpenter S. 2020. The how and why of lncRNA function: An innate immune perspective. Biochim Biophys Acta Gene Regul Mech 1863: 194419.
17. Statello L, Guo C-J, Chen L-L, and Huarte M. 2021. Gene regulation by long non-coding RNAs and its biological functions. Nat Rev Mol Cell Biol 22: 96–118. [PubMed: 33353982]
18. Quinn JJ, and Chang HY 2016. Unique features of long non-coding RNA biogenesis and function. Nat Rev Genet 17: 47–62. [PubMed: 26666209]
19. Aftabi Y, Ansarin K, Shanehbandi D, Khalili M, Seyedrezazadeh E, Rahbarnia L, Asadi M, Amiri-Sadeghan A, Zafari V, Eyvazi S, Bakhtiyari N, and Zarredar H. 2021. Long non-coding RNAs as potential biomarkers in the prognosis and diagnosis of lung cancer: A review and target analysis. IUBMB Life 73: 307–327. [PubMed: 33369006]
20. Ma T, Jia H, Ji P, He Y, and Chen L. 2021. Identification of the candidate lncRNA biomarkers for acute kidney injury: a systematic review and meta-analysis. Expert Rev Mol Diagn 21: 77–89. [PubMed: 33612038]
21. Viereck J, and Thum T. 2017. Circulating Noncoding RNAs as Biomarkers of Cardiovascular Disease and Injury. Circ Res 120: 381–399. [PubMed: 28104771]
22. Teng X, Liao J, Zhao L, Dong W, Xue H, Bai L, and Xu S. 2021. Whole transcriptome analysis of the differential RNA profiles and associated competing endogenous RNA networks in LPS-induced acute lung injury (ALI). PLoS One 16: e0251359.
23. Wang J, Shen Y-C, Chen Z-N, Yuan Z-C, Wang H, Li D-J, Liu K, and Wen F-Q 2019. Microarray profiling of lung long non-coding RNAs and mRNAs in lipopolysaccharide-induced acute lung injury mouse model. Biosci Rep 39: BSR20181634.
24. Chen C, He Y, Feng Y, Hong W, Luo G, and Ye Z. 2021. Long non-coding RNA review and implications in acute lung inflammation. Life Sci 269: 119044.
25. Asti C, Ruggieri V, Porzio S, Chiusaroli R, Melillo G, and Caselli GF 2000. Lipopolysaccharide-induced lung injury in mice. I. Concomitant evaluation of inflammatory cells and haemorrhagic lung damage. Pulm Pharmacol Ther 13: 61–69. [PubMed: 10799283]
26. Dai L, Zhang G, Cheng Z, Wang X, Jia L, Jing X, Wang H, Zhang R, Liu M, Jiang T, Yang Y, and Yang M. 2018. Knockdown of LncRNA MALAT1 contributes to the suppression of inflammatory responses by up-regulating miR-146a in LPS-induced acute lung injury. Connect Tissue Res 59: 581–592. [PubMed: 29649906]
27. Li J, Xue L, Wu Y, Yang Q, Liu D, Yu C, and Peng J. 2021. STAT3-activated lncRNA XIST accelerates the inflammatory response and apoptosis of LPS-induced acute lung injury. J Cell Mol Med.
28. Carpenter S, Aiello D, Atianand MK, Ricci EP, Gandhi P, Hall LL, Byron M, Monks B, Henry-Bezy M, Lawrence JB, O'Neill LAJ, Moore MJ, Caffrey DR, and Fitzgerald KA 2013. A long noncoding RNA mediates both activation and repression of immune response genes. Science 341: 789–792. [PubMed: 23907535]
29. Tong Q, Gong A-Y, Zhang X-T, Lin C, Ma S, Chen J, Hu G, and Chen X-M 2016. LincRNA-Cox2 modulates TNF-α-induced transcription of Il12b gene in intestinal epithelial cells through

regulation of Mi-2/NuRD-mediated epigenetic histone modifications. FASEB J 30: 1187–1197. [PubMed: 26578685]

30. Hu G, Gong A-Y, Wang Y, Ma S, Chen X, Chen J, Su C-J, Shibata A, Strauss-Soukup JK, Drescher KM, and Chen X-M 2016. LincRNA-Cox2 Promotes Late Inflammatory Gene Transcription in Macrophages through Modulating SWI/SNF-Mediated Chromatin Remodeling. J Immunol 196: 2799–2808. [PubMed: 26880762]
31. Covarrubias S, Robinson EK, Shapleigh B, Vollmers A, Katzman S, Hanley N, Fong N, McManus MT, and Carpenter S. 2017. CRISPR/Cas-based screening of long non-coding RNAs (lncRNAs) in macrophages with an NF-κB reporter. J Biol Chem 292: 20911–20920.
32. Hu G, Liao K, Niu F, Yang L, Dallon BW, Callen S, Tian C, Shu J, Cui J, Sun Z, Lyubchenko YL, Ka M, Chen X-M, and Buch S. 2018. Astrocyte EV-Induced lincRNA-Cox2 Regulates Microglial Phagocytosis: Implications for Morphine-Mediated Neurodegeneration. Mol Ther Nucleic Acids 13: 450–463. [PubMed: 30388619]
33. Liao K, Niu F, Dagur RS, He M, Tian C, and Hu G. 2020. Intranasal Delivery of lincRNA-Cox2 siRNA Loaded Extracellular Vesicles Decreases Lipopolysaccharide-Induced Microglial Proliferation in Mice. J Neuroimmune Pharmacol 15: 390–399. [PubMed: 31325121]
34. Xue Z, Zhang Z, Liu H, Li W, Guo X, Zhang Z, Liu Y, Jia L, Li Y, Ren Y, Yang H, Zhang L, Zhang Q, Da Y, Hao J, Yao Z, and Zhang R. 2019. lincRNA-Cox2 regulates NLRP3 inflammasome and autophagy mediated neuroinflammation. Cell Death Differ 26: 130–145. [PubMed: 29666475]
35. Sauvageau M, Goff LA, Lodato S, Bonev B, Groff AF, Gerhardinger C, Sanchez-Gomez DB, Hacisuleyman E, Li E, Spence M, Liapis SC, Mallard W, Morse M, Swerdel MR, D'Ecclessis MF, Moore JC, Lai V, Gong G, Yancopoulos GD, Frendewey D, Kellis M, Hart RP, Valenzuela DM, Arlotta P, and Rinn JL 2013. Multiple knockout mouse models reveal lincRNAs are required for life and brain development. Elife 2: e01749.
36. Elling R, Robinson EK, Shapleigh B, Liapis SC, Covarrubias S, Katzman S, Groff AF, Jiang Z, Agarwal S, Motwani M, Chan J, Sharma S, Hennessy EJ, FitzGerald GA, McManus MT, Rinn JL, Fitzgerald KA, and Carpenter S. 2018. Genetic Models Reveal cis and trans Immune-Regulatory Activities for lincRNA-Cox2. Cell Rep 25: 1511–1524.e6.
37. Tasic B, Hippenmeyer S, Wang C, Gamboa M, Zong H, Chen-Tsai Y, and Luo L. 2011. Site-specific integrase-mediated transgenesis in mice via pronuclear injection. Proc Natl Acad Sci U S A 108: 7902–7907. [PubMed: 21464299]
38. Allen IC 2014. The utilization of oropharyngeal intratracheal PAMP administration and bronchoalveolar lavage to evaluate the host immune response in mice. J Vis Exp.
39. Nielsen TB, Yan J, Luna B, and Spellberg B. 2018. Murine Oropharyngeal Aspiration Model of Ventilator-associated and Hospital-acquired Bacterial Pneumonia. J Vis Exp.
40. Ehrentraut H, Weisheit CK, Frede S, and Hilbert T. 2019. Inducing Acute Lung Injury in Mice by Direct Intratracheal Lipopolysaccharide Instillation. J Vis Exp.
41. Poscablo DM, Worthington AK, Smith-Berdan S, and Forsberg EC 2021. Megakaryocyte progenitor cell function is enhanced upon aging despite the functional decline of aged hematopoietic stem cells. Stem Cell Reports 16: 1598–1613. [PubMed: 34019813]
42. Cloonan SM, Glass K, Laucho-Contreras ME, Bhashyam AR, Cervo M, Pabón MA, Konrad C, Polverino F, Siempos II, Perez E, Mizumura K, Ghosh MC, Parameswaran H, Williams NC, Rooney KT, Chen Z-H, Goldklang MP, Yuan G-C, Moore SC, Demeo DL, Rouault TA, D'Armiento JM, Schon EA, Manfredi G, Quackenbush J, Mahmood A, Silverman EK, Owen CA, and Choi AMK 2016. Mitochondrial iron chelation ameliorates cigarette smoke-induced bronchitis and emphysema in mice. Nat Med 22: 163–174. [PubMed: 26752519]
43. Robinson EK, Covarrubias S, Zhou S, and Carpenter S. 2021. Generation and utilization of a HEK-293T murine GM-CSF expressing cell line. PLoS One 16: e0249117.
44. Chen BD, Mueller M, and Chou TH 1988. Role of granulocyte/macrophage colony-stimulating factor in the regulation of murine alveolar macrophage proliferation and differentiation. J Immunol 141: 139–144. [PubMed: 3288696]
45. Yu Y-RA, O'Koren EG, Hotten DF, Kan MJ, Kopin D, Nelson ER, Que L, and Gunn MD 2016. A Protocol for the Comprehensive Flow Cytometric Analysis of Immune Cells in Normal and Inflamed Murine Non-Lymphoid Tissues. PLoS One 11: e0150606.

46. Nakano H, Nakano K, and Cook DN 2018. Isolation and Purification of Epithelial and Endothelial Cells from Mouse Lung. Methods Mol Biol 1799: 59–69. [PubMed: 29956144]
47. Mould KJ, Barthel L, Mohning MP, Thomas SM, McCubbrey AL, Danhorn T, Leach SM, Fingerlin TE, O'Connor BP, Reisz JA, D'Alessandro A, Bratton DL, Jakubzick CV, and Janssen WJ 2017. Cell Origin Dictates Programming of Resident versus Recruited Macrophages during Acute Lung Injury. Am J Respir Cell Mol Biol 57: 294–306. [PubMed: 28421818]
48. Mould KJ, Jackson ND, Henson PM, Seibold M, and Janssen WJ 2019. Single cell RNA sequencing identifies unique inflammatory airspace macrophage subsets. JCI Insight 4: 126556.
49. Riemondy KA, Jansing NL, Jiang P, Redente EF, Gillen AE, Fu R, Miller AJ, Spence JR, Gerber AN, Hesselberth JR, and Zemans RL 2019. Single cell RNA sequencing identifies TGFβ as a key regenerative cue following LPS-induced lung injury. JCI Insight 5: 123637.
50. Wolf FA, Angerer P, and Theis FJ 2018. SCANPY: large-scale single-cell gene expression data analysis. Genome Biol 19: 15. [PubMed: 29409532]
51. Hashimoto D, Chow A, Noizat C, Teo P, Beasley MB, Leboeuf M, Becker CD, See P, Price J, Lucas D, Greter M, Mortha A, Boyer SW, Forsberg EC, Tanaka M, van Rooijen N, García-Sastre A, Stanley ER, Ginhoux F, Frenette PS, and Merad M. 2013. Tissue-resident macrophages self-maintain locally throughout adult life with minimal contribution from circulating monocytes. Immunity 38: 792–804. [PubMed: 23601688]
52. Domscheit H, Hegeman MA, Carvalho N, and Spieth PM 2020. Molecular Dynamics of Lipopolysaccharide-Induced Lung Injury in Rodents. Front Physiol 11: 36. [PubMed: 32116752]
53. Ali H, Khan A, Ali J, Ullah H, Khan A, Ali H, Irshad N, and Khan S. 2020. Attenuation of LPS-induced acute lung injury by continentalic acid in rodents through inhibition of inflammatory mediators correlates with increased Nrf2 protein expression. BMC Pharmacol Toxicol 21: 81. [PubMed: 33239093]
54. Menon M, Hussell T, and Ali Shuwa H. 2021. Regulatory B cells in respiratory health and diseases. Immunol Rev 299: 61–73. [PubMed: 33410165]
55. Seys LJM, Verhamme FM, Schinwald A, Hammad H, Cunoosamy DM, Bantsimba-Malanda C, Sabirsh A, McCall E, Flavell L, Herbst R, Provoost S, Lambrecht BN, Joos GF, Brusselle GG, and Bracke KR 2015. Role of B Cell-Activating Factor in Chronic Obstructive Pulmonary Disease. Am J Respir Crit Care Med 192: 706–718. [PubMed: 26266827]
56. Cook PC, and MacDonald AS 2016. Dendritic cells in lung immunopathology. Semin Immunopathol 38: 449–460. [PubMed: 27256370]
57. Blázquez-Prieto J, López-Alonso I, Huidobro C, and Albaiceta GM 2018. The Emerging Role of Neutrophils in Repair after Acute Lung Injury. Am J Respir Cell Mol Biol 59: 289–294. [PubMed: 29708395]
58. Giacalone VD, Margaroli C, Mall MA, and Tirouvanziam R. 2020. Neutrophil Adaptations upon Recruitment to the Lung: New Concepts and Implications for Homeostasis and Disease. Int J Mol Sci 21: E851. [PubMed: 32013006]
59. Lee SC, Brummet ME, Shahabuddin S, Woodworth TG, Georas SN, Leiferman KM, Gilman SC, Stellato C, Gladue RP, Schleimer RP, and Beck LA 2000. Cutaneous injection of human subjects with macrophage inflammatory protein-1 alpha induces significant recruitment of neutrophils and monocytes. J Immunol 164: 3392–3401. [PubMed: 10706735]
60. Rudd JM, Pulavendran S, Ashar HK, Ritchey JW, Snider TA, Malayer JR, Marie M, Chow VTK, and Narasaraju T. 2019. Neutrophils Induce a Novel Chemokine Receptors Repertoire During Influenza Pneumonia. Front Cell Infect Microbiol 9: 108. [PubMed: 31041196]
61. Metzemaekers M, Gouwy M, and Proost P. 2020. Neutrophil chemoattractant receptors in health and disease: double-edged swords. Cell Mol Immunol 17: 433–450. [PubMed: 32238918]
62. Ramos CDL, Canetti C, Souto JT, Silva JS, Hogaboam CM, Ferreira SH, and Cunha FQ 2005. MIP-1alpha[CCL3] acting on the CCR1 receptor mediates neutrophil migration in immune inflammation via sequential release of TNF-alpha and LTB4. J Leukoc Biol 78: 167–177. [PubMed: 15831559]
63. Bonville CA, Percopo CM, Dyer KD, Gao J, Prussin C, Foster B, Rosenberg HF, and Domachowske JB 2009. Interferon-gamma coordinates CCL3-mediated neutrophil recruitment in vivo. BMC Immunol 10: 14. [PubMed: 19298652]

64. Andersen RE, Hong SJ, Lim JJ, Cui M, Harpur BA, Hwang E, Delgado RN, Ramos AD, Liu SJ, Blencowe BJ, and Lim DA 2019. The Long Noncoding RNA Pnky Is a Trans-acting Regulator of Cortical Development In Vivo. Dev Cell 49: 632–642.e7.

65. Lewandowski JP, Lee JC, Hwang T, Sunwoo H, Goldstein JM, Groff AF, Chang NP, Mallard W, Williams A, Henao-Meija J, Flavell RA, Lee JT, Gerhardinger C, Wagers AJ, and Rinn JL 2019. The Firre locus produces a trans-acting RNA molecule that functions in hematopoiesis. Nat Commun 10: 5137. [PubMed: 31723143]

66. Lewandowski JP, Dumbović G, Watson AR, Hwang T, Jacobs-Palmer E, Chang N, Much C, Turner KM, Kirby C, Rubinstein ND, Groff AF, Liapis SC, Gerhardinger C, Bester A, Pandolfi PP, Clohessy JG, Hoekstra HE, Sauvageau M, and Rinn JL 2020. The Tug1 lncRNA locus is essential for male fertility. Genome Biol 21: 237. [PubMed: 32894169]

67. Nolan A, Kwon S, Cho SJ, Naveed B, Comfort AL, Prezant DJ, Rom WN, and Weiden MD 2014. MMP-2 and TIMP-1 predict healing of WTC-lung injury in New York City firefighters. Respir Res 15: 5. [PubMed: 24447332]

68. Chen G, Ge D, Zhu B, Shi H, and Ma Q. 2020. Upregulation of matrix metalloproteinase 9 (MMP9)/tissue inhibitor of metalloproteinase 1 (TIMP1) and MMP2/TIMP2 ratios may be involved in lipopolysaccharide-induced acute lung injury. J Int Med Res 48: 300060520919592.

69. Davey A, McAuley DF, and O'Kane CM 2011. Matrix metalloproteinases in acute lung injury: mediators of injury and drivers of repair. Eur Respir J 38: 959–970. [PubMed: 21565917]

70. Beck-Schimmer B, Schwendener R, Pasch T, Reyes L, Booy C, and Schimmer RC 2005. Alveolar macrophages regulate neutrophil recruitment in endotoxin-induced lung injury. Respir Res 6: 61. [PubMed: 15972102]

71. Herold S, Mayer K, and Lohmeyer J. 2011. Acute lung injury: how macrophages orchestrate resolution of inflammation and tissue repair. Front Immunol 2: 65. [PubMed: 22566854]

72. Machiels B, Dourcy M, Xiao X, Javaux J, Mesnil C, Sabatel C, Desmecht D, Lallemand F, Martinive P, Hammad H, Guilliams M, Dewals B, Vanderplasschen A, Lambrecht BN, Bureau F, and Gillet L. 2017. A gammaherpesvirus provides protection against allergic asthma by inducing the replacement of resident alveolar macrophages with regulatory monocytes. Nat Immunol 18: 1310–1320. [PubMed: 29035391]

73. Nayak DK, Mendez O, Bowen S, and Mohanakumar T. 2018. Isolation and In Vitro Culture of Murine and Human Alveolar Macrophages. J Vis Exp.

74. Kobayashi Y. 2008. The role of chemokines in neutrophil biology. Front Biosci 13: 2400–2407. [PubMed: 17981721]

75. Guilliams M, De Kleer I, Henri S, Post S, Vanhoutte L, De Prijck S, Deswarte K, Malissen B, Hammad H, and Lambrecht BN 2013. Alveolar macrophages develop from fetal monocytes that differentiate into long-lived cells in the first week of life via GM-CSF. J Exp Med 210: 1977–1992. [PubMed: 24043763]

76. Misharin AV, Morales-Nebreda L, Reyfman PA, Cuda CM, Walter JM, McQuattie-Pimentel AC, Chen C-I, Anekalla KR, Joshi N, Williams KJN, Abdala-Valencia H, Yacoub TJ, Chi M, Chiu S, Gonzalez-Gonzalez FJ, Gates K, Lam AP, Nicholson TT, Homan PJ, Soberanes S, Dominguez S, Morgan VK, Saber R, Shaffer A, Hinchcliff M, Marshall SA, Bharat A, Berdnikovs S, Bhorade SM, Bartom ET, Morimoto RI, Balch WE, Sznajder JI, Chandel NS, Mutlu GM, Jain M, Gottardi CJ, Singer BD, Ridge KM, Bagheri N, Shilatifard A, Budinger GRS, and Perlman H. 2017. Monocyte-derived alveolar macrophages drive lung fibrosis and persist in the lung over the life span. J Exp Med 214: 2387–2404. [PubMed: 28694385]

77. Collins MK, Shotland AM, Wade MF, Atif SM, Richards DK, Torres-Llompart M, Mack DG, Martin AK, Fontenot AP, and McKee AS 2020. A role for TNF-α in alveolar macrophage damage-associated molecular pattern release. JCI Insight 5: 134356.

78. Gangwar RS, Vinayachandran V, Rengasamy P, Chan R, Park B, Diamond-Zaluski R, Cara EA, Cha A, Das L, Asase C, Maiseyeu A, Deiuliis J, Zhong J, Mitzner W, Biswal S, and Rajagopalan S. 2020. Differential contribution of bone marrow-derived infiltrating monocytes and resident macrophages to persistent lung inflammation in chronic air pollution exposure. Sci Rep 10: 14348.

Key Points

- *lincRNA-Cox2* is highly expressed in the lung and most inducible in AMs following LPS
- We show *lincRNA-Cox2* functions in *trans* to regulate gene expression following ALI
- *lincRNA-Cox2's* function is mediated by BM derived cells, likely infiltrating AMs

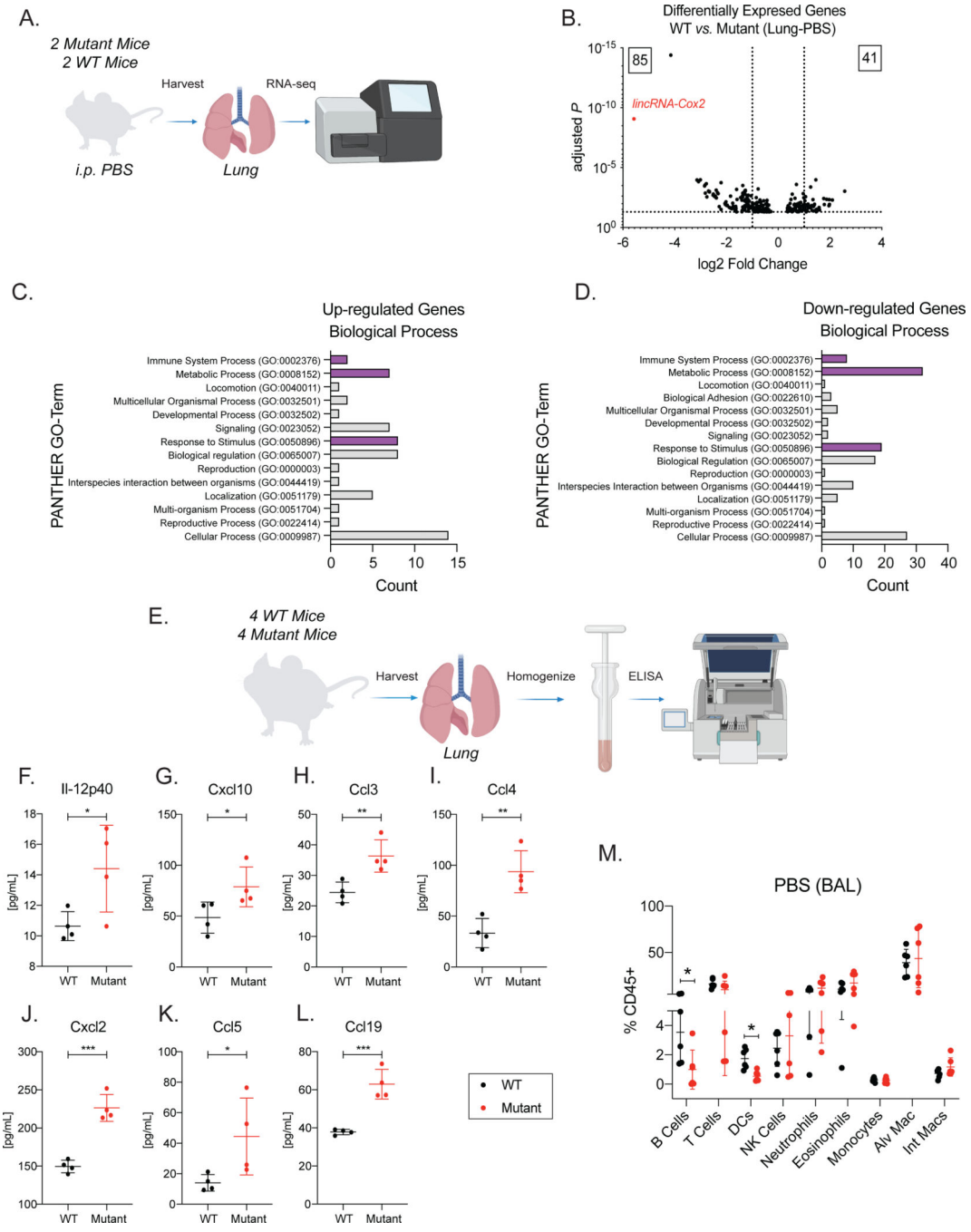

Figure 1: *lincRNA-Cox2* regulates immune signaling within the lung during homeostasis.

(A) Schematic of RNA-seq analysis of WT and Mutant lungs at baseline. (B) Volcano plot of differentially expressed genes from WT *vs.* Mutant lungs. Biological process gene ontology of (C) up-regulated genes and (D) down-regulated genes. (E) Schematic of cytokine analysis of lung homogenates from WT and mutant mice. Multiplex cytokine analysis was performed on lung homogenates for (F) Il-12p40 (G) Cxcl10 (H) Ccl3 (I) Ccl4 (J) Cxcl2 (K) Ccl5 and (L) Ccl19. (M) Flow cytometry analysis of immune cells in the bronchiolar lavage fluid (BAL) at baseline gated on CD45+ cells. The student's t-test used

to determine the significance between WT and mutant mice. Asterisks indicate statistical significance (*=> 0.05, **>=.01, ***=> 0.0005).

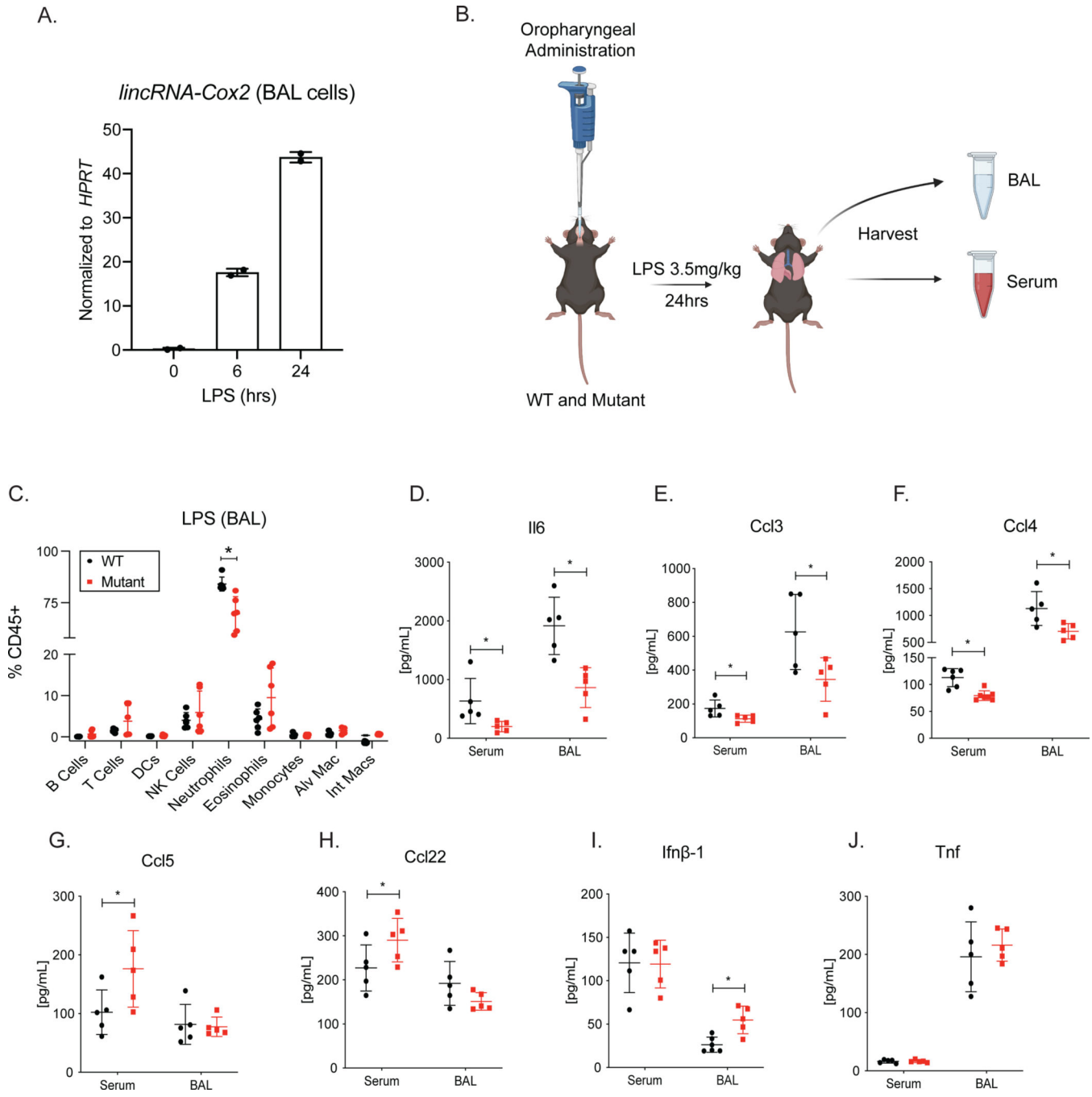

Figure 2: *lincRNA-Cox2* positively regulates the pro-inflammatory response during acute lung injury (ALI).

(A) 6 WT mice were treated with either PBS or 3.5mg/kg of LPS via the oropharyngeal route. After 6h and 24h, BALs were harvested, and RNA was isolated. *lincRNA-Cox2* was measured by RT-qPCR in pooled BAL cells. (B) ALI schematic depicting the oropharyngeal route of 3.5mg/kg LPS administration in WT and Mutant. Mice were sacrificed after 24 h, followed by harvesting serum and bronchiolar lavage fluid (BAL). (C) BAL cells were analyzed by flow cytometry to assess recruitment of immune cells in WT and immune cells gated off CD45+. Multiplex cytokine analysis was performed on serum and BAL for (D)

Il6, (E) Ccl5, (F) Ccl3, (G) Ccl4, (H) Ccl22, (I) Ifnb-1 and (J) Tnf. The student's t-test used to determine the significance between WT and mutant mice. Asterisks indicate statistical significance (*=> 0.05, **>=.01, ***=> 0.0005).

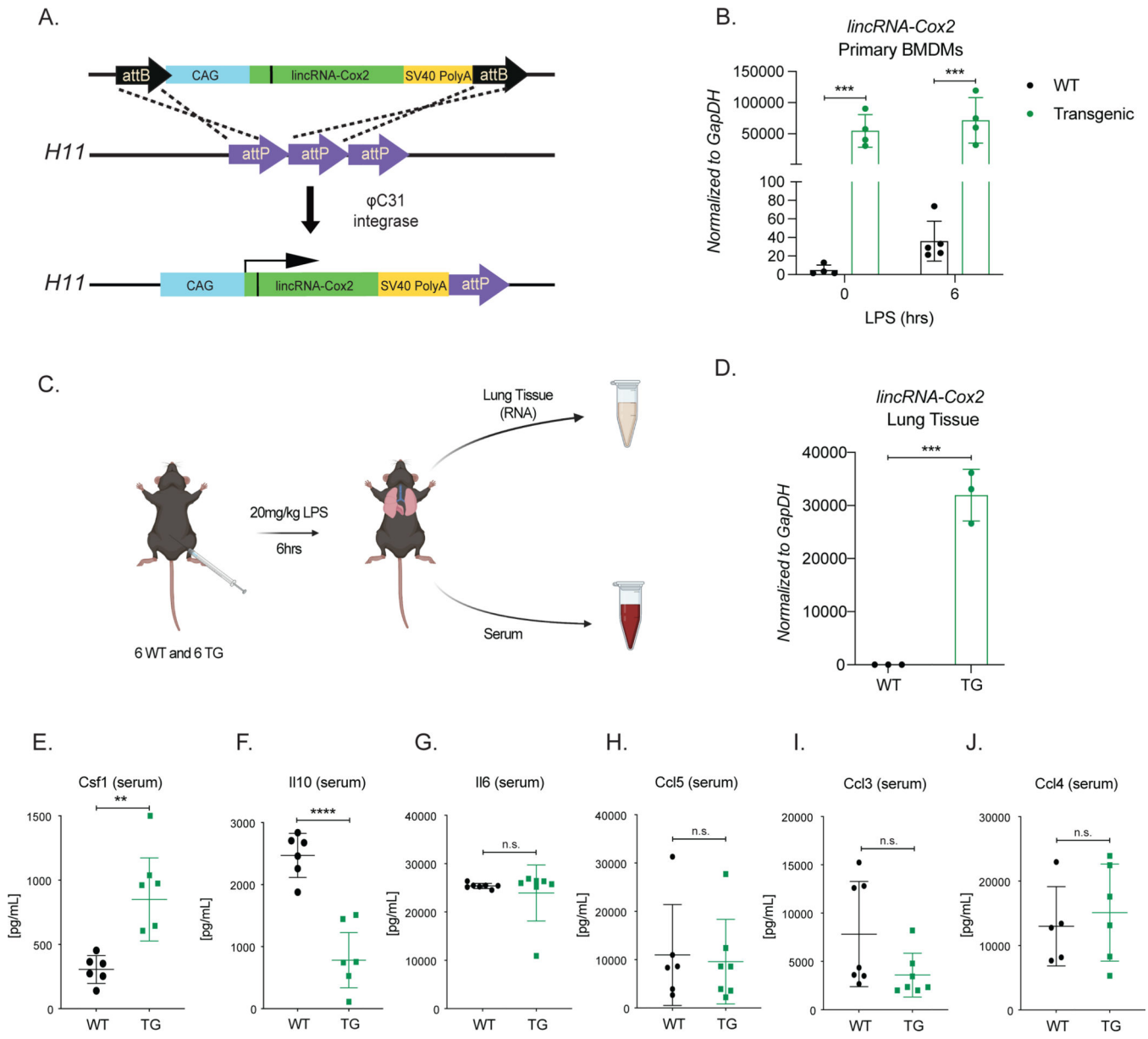

Figure 3: Characterization of *lincRNA-Cox2* transgenic mouse.

(A) We have generated a transgenic *lincRNA-Cox2* mouse line using the TARGATT system. This approach allows for stable integration of *lincRNA-Cox2* into the H11 locus. Our inserted cassette is carrying a CAG promoter, *lincRNA-Cox2*, and an SV40 polA stop cassette. (B) *lincRNA-Cox2* levels measured in WT and Transgenic bone-marrow-derived macrophages with and without LPS for 6 h, normalized to GapDH. (C) Schematic of 20mg/kg LPS septic shock model of WT and transgenic mice. (D) lincRNA-Cox2 measured by RT-qPCR in lung tissue. Serum was harvested and ELISAs were performed to measure (E) Csf1, (F) Il10, (G) Il6, (H) Ccl5, (I) Ccl3 and (J) Ccl4. The student's t-test used to determine the significance between WT and TG mice. Asterisks indicate statistical significance (*=> 0.05, **>=.01, ***=> 0.0005).

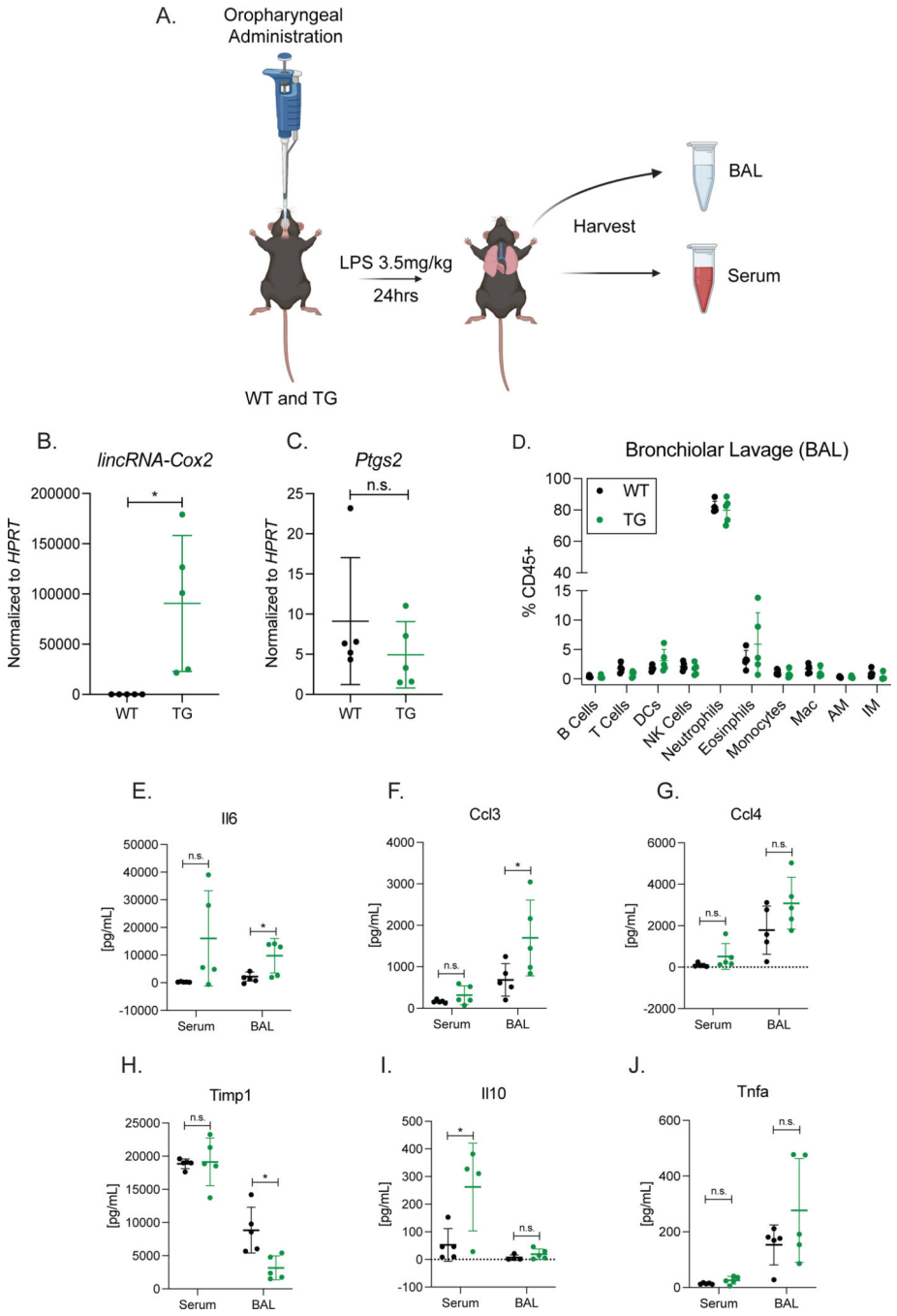

Figure 4: Over-expression of *lincRNA-Cox2* heightens inflammation during ALI.

(A) ALI schematic depicting the oropharyngeal route of 3.5mg/kg LPS administration in WT and TG. Mice were sacrificed after 24 h, followed by harvesting serum and BAL fluid. (B) *lincRNA-Cox2* and (C) Ptgs2 measured by RT-qPCR in BAL cells. (D) BAL cells were analyzed by flow cytometry to assess recruitment of immune cells in WT and immune cells gated off CD45+. Multiplex cytokine analysis was performed on serum and BAL for (E) Il6, (F) Ccl3, (G) Ccl4, (H) Timp1, (I) Il10, (J) Tnfa. Student's t-test used

to determine significance and asterisks indicate statistical significance (*=> 0.05, **>=.01, ***=> 0.0005).

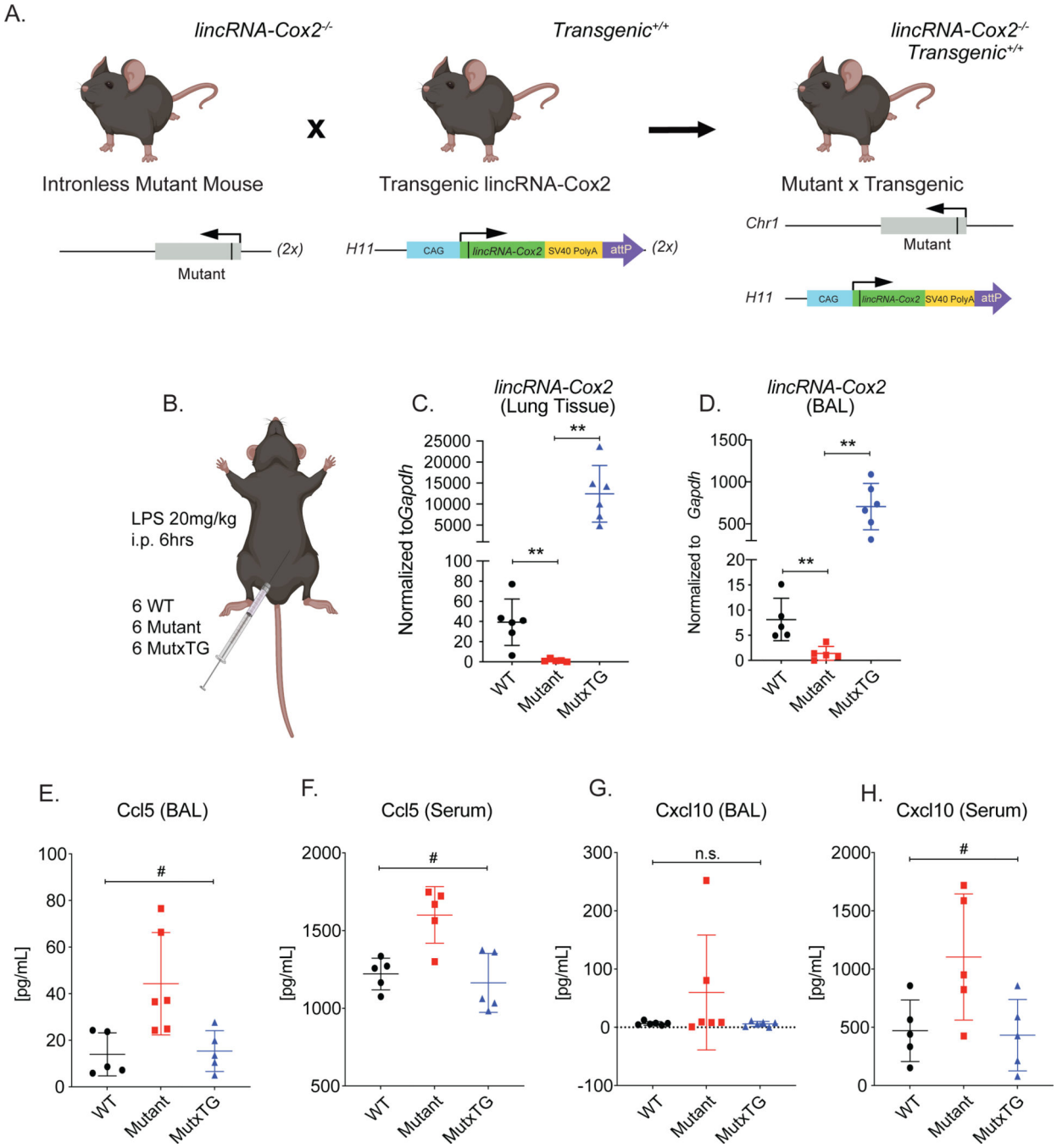

Figure 5: *lincRNA-Cox2* functions in *trans* to regulate the innate immune system in a septic shock model.

(A) Schematic depicting i.p. route of LPS infection in WT, mutant and transgenic mice. (C) WT, Mutant and TgxMut mice were challenged with 20mg/kg LPS and body temperatures were measured. Mice were sacrificed after 6h, bronchiolar lavage fluid (BAL), lungs and cardiac punctures were performed. BAL and Lungs were harvested for gene expression analysis by RT-qPCR for *lincRNA-Cox2* (C-D), Ccl5 (E-F). BAL and isolated serum were sent for multiplex cytokine analysis (G-H). Each dot represents an individual animal. Student's t-tests were performed using Graphpad Prism7. Asterisks indicate statistically

significant differences between mouse lines (*= >0.05, **= >0.01 and *** = >0.005). One-way ANOVA used to determine significance between WT, Mut, and MutxTG mice (#=>0.05).

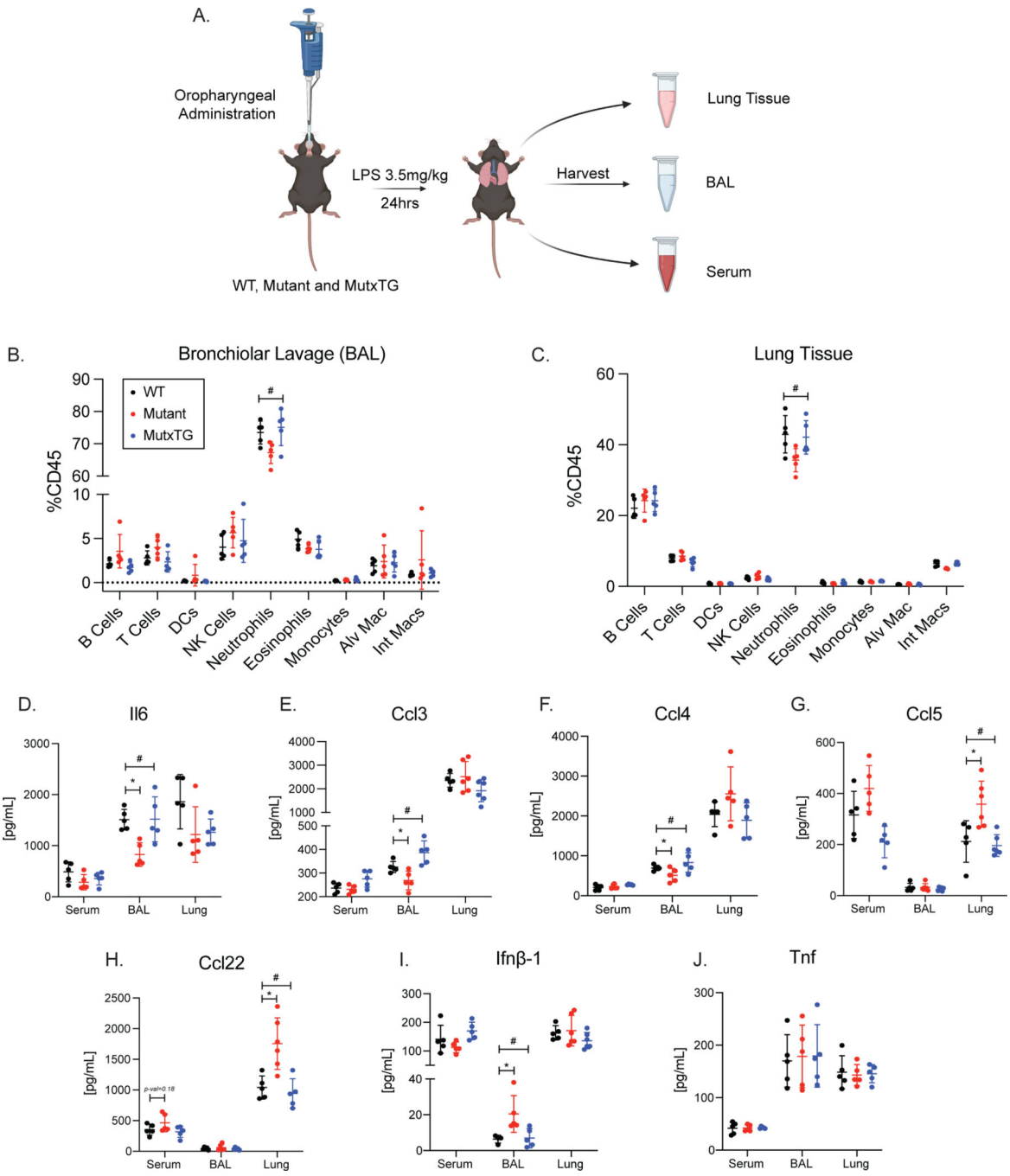

Figure 6: *lincRNA-Cox2* regulates the proinflammatory response in the lung in *trans*.

(A) Generation of *lincRNA-Cox2* MutxTG homozygous mouse. (B) ALI schematic depicting the oropharyngeal route of 3.5mg/kg LPS administration in WT, Mutant, and MutxTG. Mice were sacrificed after 24 h, followed by harvesting lung tissue, serum, and BAL fluid. (C) BAL and (D) Lung cells were analyzed by flow cytometry to assess recruitment of immune cells in WT and immune cells gated off CD45+. Multiplex cytokine analysis was performed on serum, BAL, and Lung tissue for (E) Il6, (F) Ccl5, (G) Ccl3, (H) Ccl4, (I) Ccl22, (J) Ifnb1 and (K) Tnf. Student's t-test used to determine significance

between WT and Mut mice (*=> 0.05). One-way ANOVA used to determine significance between WT, Mut, and MutxTG mice (#=>0.05).

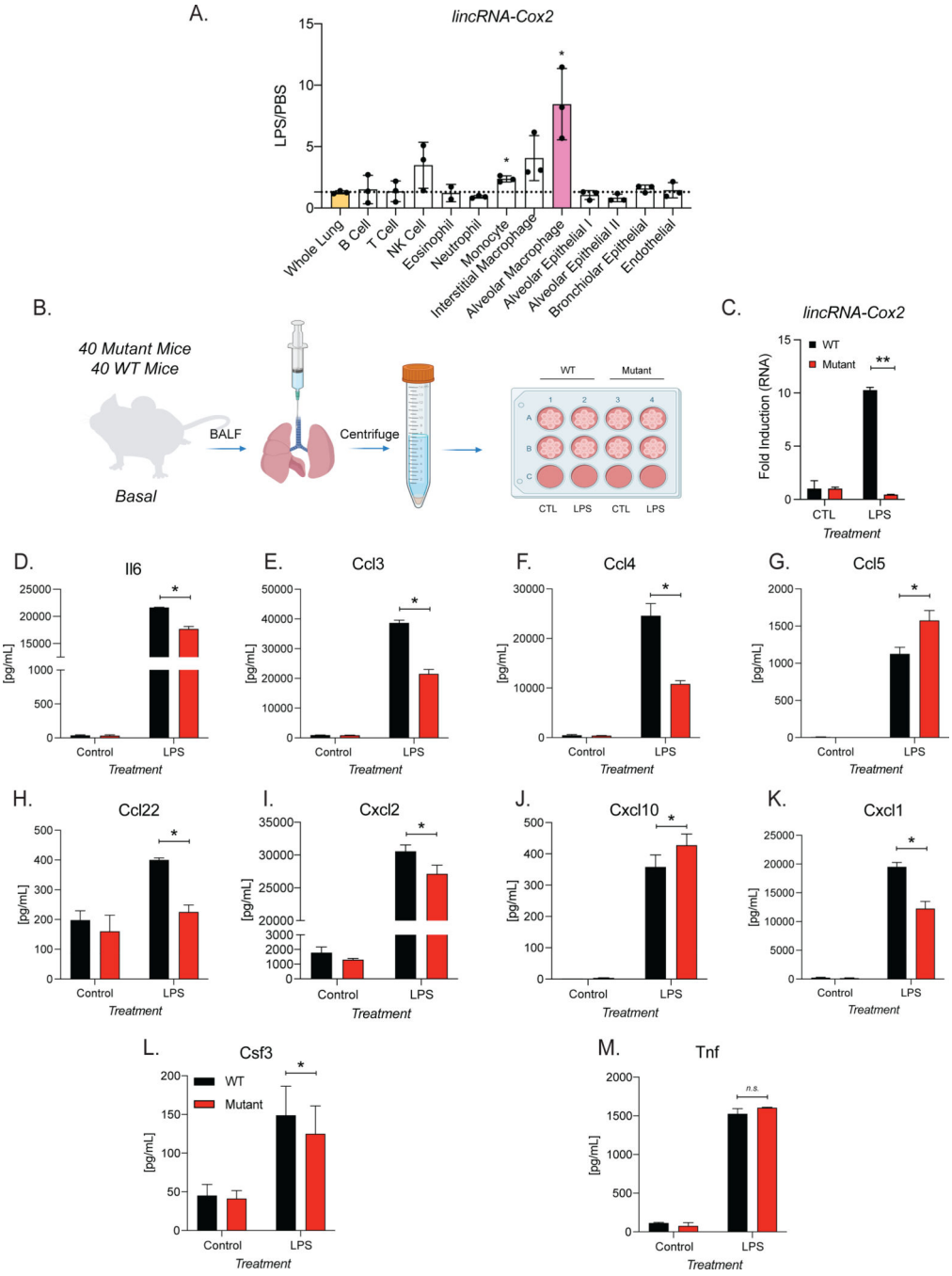

Figure 7: *lincRNA-Cox2* is inducible and regulates immune genes both positively and negatively in primary alveolar macrophages.

(A) *lincRNA-Cox2* was measured in whole lung tissue and several sorted immune and epithelial cells from mice treated with PBS and LPS via an oropharyngeal route. Expression was normalized to PBS. Performed in biological triplicates and student's t-test was performed between whole lung tissue and each sorted cell. (B) The experimental design is depicted. BALs harvested from 40 WT and 40 Mutant mice, 10 WT or Mutant mice were pooled per well. Cells were treated with LPS for 24 h. (C) *lincRNA-Cox2* was measured by RT-qPCR in primary alveolar macrophages. Multiplex cytokine analysis was

performed supernatant from primary alveolar macrophages for (D) Il6, (E) Ccl5, (F) Ccl3, (G) Ccl4, (H) Ccl22, (I) Ccl2, (J) Cxcl10 and (K) Cxcl1. Student's t-test used to determine significance and asterisks indicate statistical significance (*=> 0.05, **>=.01, ***=> 0.0005).

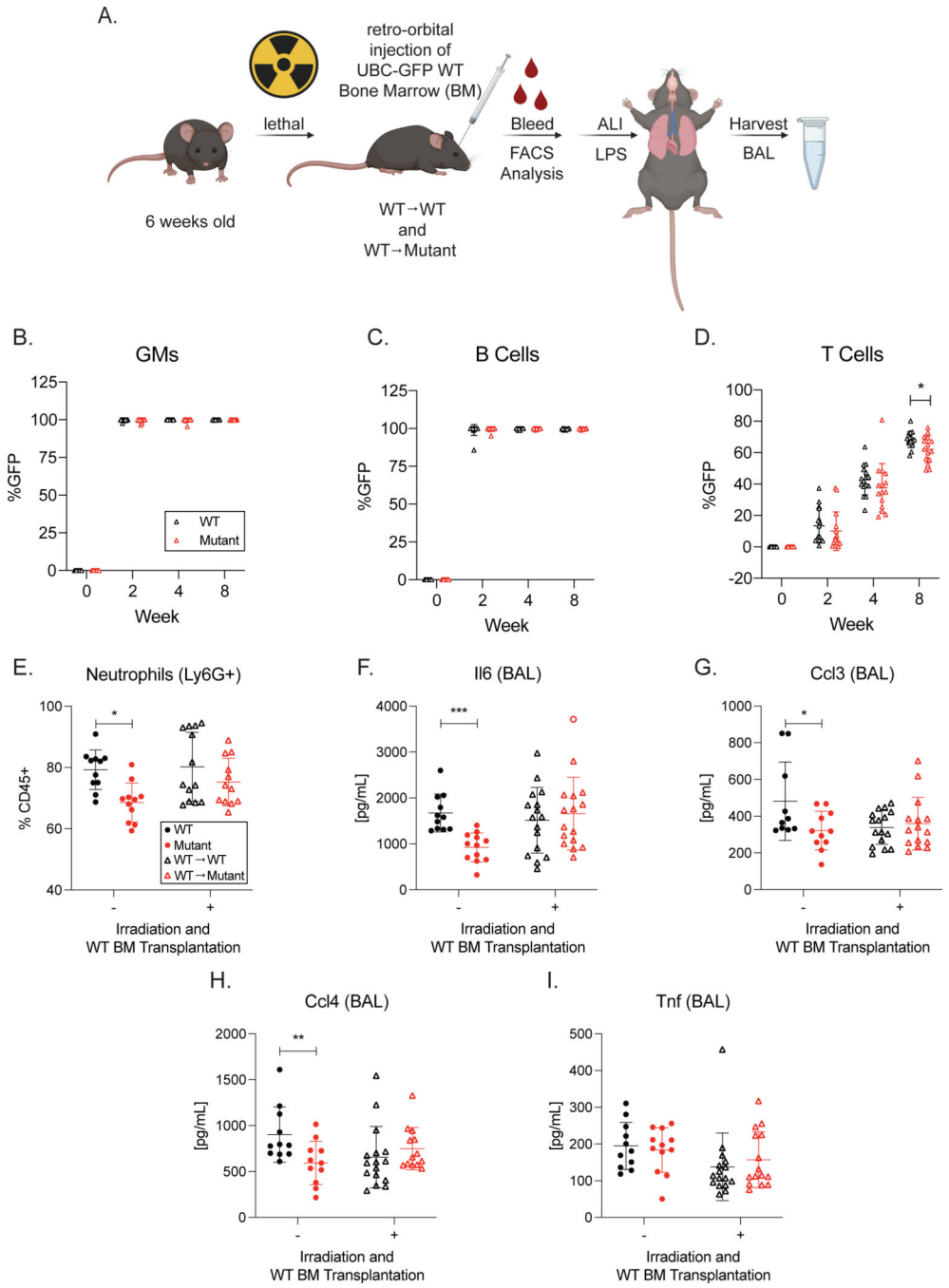

Figure 8: WT Bone marrow transplantation in *lincRNA-Cox2* mutant mice rescues the ALI phenotype.

(A) WT bone marrow transplantation and ALI experiment schematic. Chimerism was assessed in the peripheral blood by gating for GFP% of (B) granulocytes/myelomonocytes (GMs), (C) B cells and (D) T cells. (E) Percentage of Ly6G+ neutrophil populations were graphed of WT, Mutant, WT→WT and WT→Mut mice. Multiplex cytokine analysis was performed on BAL for (F) Il6, (G) Ccl3, (H) Ccl4 and (I) Tnf. Data of non-bone marrow transplant (BMT) mice experiments are from Figures 2 and 5. Student's t-test used to

determine significance and asterisks indicate statistical significance (*=> 0.05, **>=.01, ***=> 0.0005).